Supporting Information:

Mechanochromic Double Network Hydrogels as a Compression Stress Sensor

Che-Hao Wu,[†a] Cheng-Wei Tu,[†b] Junko Aimi,[c] Jiawei Zhang,[d] Tao Chen,[d] Chung-Chi Wang[e] and Chih-Feng Huang*[a]

[a] C. H. Wu, Prof. C. F. Huang*
Department of Chemical Engineering, i-Center for Advanced Science and Technology (*i*CAST), National Chung Hsing University, 145 Xingda Road, South District, Taichung 40227, Taiwan. E-mail: HuangCF@dragon.nchu.edu.tw

[b] Dr. C. W. Tu
Industrial Technology Research Institute, 195, Sec. 4, Chung Hsing Road, Chutung, Hsinchu 31057, Taiwan.

[c] Dr. J. Aimi
Research Center for Functional Materials, National Institute for Materials Science, 1-2-1 Sengen, Tsukuba, Ibaraki 305-0047, Japan.

[d] Prof. Zhang, Prof. Chen
Key Laboratory of Marine Materials and Related Technologies, Zhejiang Key, Laboratory of Marine Materials and Protective Technologies, Ningbo Institute of Material Technology and Engineering, Chinese Academy of Sciences, Ningbo, 315201, China.

[e] Dr. Chung-Chi Wang
Division of Cardiovascular Surgery, Veterans General Hospital, 40705 Taichung, Taiwan.

[†] C. H. Wu and C. W. Tu contributed equally to this work as first authors.

Captions

Experimental section

Experimental section

Materials. Rhodamine 6G (Rh–6G, 99%, ACROS), ethanolamine (99%, ACROS), 2-chloroethanol (99%, ACROS), acrylic acid (AA, 98%, ACROS), TWEEN 80 (>95 wt%, ACROS) tetramethylethylenediamine (TMEDA, 99%, Alfa Aesar), acryloyl chloride (96%, Alfa Aesar), acrylamido-2-methylpropane sulfonic acid (AMPS, 98%, Alfa Aesar), *N,N*′-methylenebisacrylamide (NMBA, 97%, Alfa Aesar), *N,N*-dimethylacrylamide (DMAA, 99%, Sigma-Aldrich), triethylamine (99.5%, Sigma-Aldrich), ammonium persulfate (APS, 98%, SHOWA), magnesium sulfate anhydrous ($MgSO_4$, 99%, SHOWA), dichloromethane (DCM, 99.5%, ECHO), acetonitrile (99.9%, ECHO), ethanol (99.5%, ECHO), and potassium carbonate (K_2CO_3, 99%, J.T Baker) were used as received without further purification.

Characterizations. The mechanical properties were tested by universal testing machine. For the tensile test of hydrogels, the universal testing machine (Cometech QC-513A2) was used for recording the stress-strain curve of DN hydrogels having a dumb-bell shape with the gauge length, width, and thickness of 50 mm, 4 mm, and 2.5 mm, respectively. The tensile speed was controlled at 25 mm/min during the test. The compression data of DN and Rh–DN hydrogels was collected by another universal testing machine (GOTECH AI-7000S). The sample for compression test was cut into a cylindrical specimen with the diameter of 10 mm and thickness of 5 mm. The compressive speed was controlled at 0.5 mm/min. Differential scanning calorimetry (DSC) was performed under a continuous nitrogen purge (30 mL/min) using a TA Instruments DSC Q10. All samples were first heated to 200 °C at a ramp rate of 10 °C/min, maintained isothermally for 5 min, and cooled down to 30 °C at ramp rate of –20 °C/min. Data were gathered on the second heating cycle at a scan rate of 10 °C/min over the temperature ranging from 30 to 200 °C. The glass transition temperature (T_g) was taken as the midpoint of the heat capacity transition between the upper and lower points of the deviation from the extrapolated glass and liquid lines. Thermal gravimetric analyses (TGA) were performed under N_2 using a TA Instruments TGA Q50 at a heating rate of 10 °C/min and recorded the weight data from 120 °C to 800 °C. The thermal decomposition temperature ($T_{d5\%}$) was taken as the 5% weight loss of the dried sample during heating. The UV–Vis absorption spectra of hydrogel samples was measured by a UV-Visible spectrophotometer (Thermo Scientific™ BioMate™ 3 Series Spectrophotometers). The apparent images were calibrated by standard white balance method to correct the colour by image software. The ^1H NMR spectra were recorded in $CDCl_3$ on Varian NMR spectrometer (Unity INOVA 400, 400 MHz) and used the residual internal $CDCl_3$ signal as a standard. The cross section morphologies of hydrogels were token by thermal field rmission scanning electron microscope with cryo system (FE-SEM JEOL JSM-7800F/Quorum Technologies PP3010T Cryo-SEM Preparation System). Fourier-transfer infrared (FT-IR) spectra of Rh–TA and dried hydrogel samples were recorded by an attenuated

total refraction FT-IR Spectrometer (PerkinElmer FT-IR SP-1). The light scattering of emulsified solutions was recorded by a dynamic light scattering (DLS) analyser (NanoBrook ZetaPALS).

Synthesis of Rh–2NH (i.e., step (i) in Scheme S2). Rh–6G (5.00 g, 10.44 mmol) was dissolved in 84.1 mL of acetonitrile (1.53 mol) with vigorous stirring in a Schlenk flask, and then ethanolamine (1.89 mL, 31.31 mmol) was slowly added in to the mixture solution to reach a homogeneous solution. The reaction solution was put into an oil bath at temperature of 90 °C and refluxed for few hours. After the reaction cooled down, the aqueous phase was removed by filtration method and the precipitate was collected. After evaporating residual solvents in a vacuum, a mahogany powder of Rh–2NH was obtained (yield: 65%; ^{1}H NMR (400 MHz, $CDCl_3$, δ = ppm): 1.33 (t, 6H), 1.92 (s, 6H), 3.22 (td, 6H), 3.46-3.42 (m, 2H), 6.32 (d, 4H), 7.06-7.00 (m, 1H), 7.46 (dd, 2H), 7.97-7.89 (m, 1H)).

Synthesis of Rh–3OH (i.e., step (ii) in Scheme S2). Rh–2NH (2.00 g, 4.36 mmol) and K_2CO_3 (4.83 g, 34.92 mmol) were added into a Schlenk flask filled with 20 mL of 2-chloroethanol (297.66 mmol) with vigorous stirring. The reaction solution was then kept at 100 °C with an oil bath and refluxed for a day. The reaction was stopped by quenching to room temperature and 2-chloroethanol was evaporated by rotary evaporation. The crude was dissolved in DCM and extracted with water three times. The organic phase was dried with $MgSO_4$ to remove residual water and crude product was obtained by evaporating DCM. The crude product was purified by column chromatography (DCM: EtOH = 35/1 (v/v)) and obtained a bright pink crystalline solid (yield: 67%; ^{1}H NMR (400 MHz, $CDCl_3$, δ = ppm): 1.02 (t, 6H), 2.10 (s, 6H), 3.02 (q, 4H), 3.21 (t, 4H), 3.31-3.25 (m, 2H), 3.47-3.43 (m, 2H), 3.61 (s, 4H), 6.49 (s, 21H), 6.90 (s, 2H), 7.04 (dd, 1H), 7.54-7.49 (m, 2H), 7.96 (dd, 1H)).

Synthesis of Rh–TA (i.e., step (iii) in Scheme S2). Rh–3OH (1.5 g, 2.75 mmol), triethylamine (3.44 mL, 24.71 mmol), and DCM (60 mL, 933 mmol) were mixed in a Schlenk flask with stirring and purged with nitrogen for an hour in an ice bath. The reaction was kept at 0 °C and slowly added with a solution of acryloyl chloride (1.33 mL, 16.47 mmol) and DCM (5 mL, 78 mmol) mixtures by using an addition funnel. After feeding, the reaction mixture was removed from ice bath and kept at room temperature with stirring for a day to complete the reaction. The reaction mixture was diluted with DCM and extracted with water three times. The organic phase was collected and dried with $MgSO_4$. After evaporating residual solvents in a vacuum, a brown powder of Rh–TA was obtained (yield: 95 %; ^{1}H NMR (400 MHz, $CDCl_3$, δ = ppm): 1.07-1.00 (m, 6H), 2.02 (d, 6H), 3.10-3.04 (m, 4H), 3.29 (t, 4H), 3.48 (t, 2H), 3.75 (t, 2H), 4.21 (t, 4H), 5.71-6.41 (m, 11H), 6.90 (d, 2H), 7.08-7.02 (m, 1H), 7.49 (dd, 2H), 8.00-7.95 (m, 1H)).

Synthesis of single network (SN) hydrogels (i.e., Scheme 1A1). AMPS and NMBA were used as monomer and crosslinker for the 1st network, respectively. AMPS (1.00 g, 4.83 mmol) and NMBA (0.03 g, 0.19 mmol) were dissolved in 4 mL of water. With additions of 1 wt% solution of TEMED (0.145 mL, 0.010 mmol) and 10 wt% solution of APS (0.165 mL, 0.072 mmol), the reaction mixture was injected into a reaction holder made by two glass plate with a space of 5 mm. Then, the 1st network hydrogel was prepared via placing the reaction holder at 50 °C for few hours.

Synthesis of double network (DN) hydrogels (i.e., Scheme 1A2). The obtaining SN hydrogel was immersed in a mixture with DMAA (3.13 mL, 30.40 mmol), AA (0.23 mL, 3.83 mmol), APS (0.099 g, 0.434 mmol), and water (12 mL). The mixture was kept in a refrigerator overnight to reach an equilibrium absorption of 2nd network reactants. DN hydrogel was then obtained through keeping the swollen SN hydrogel at 60 °C for few hours. The unreacted monomers and impurities were removed by repeat immersing the DN hydrogel in a large amount of fresh DI water three times and used with high water contents.

Synthesis of Rh-containing SN (Rh–SN) hydrogels (i.e., Scheme 1B1). For examples, TWEEN 80 (0.280 g, 0.170 mmol) and a desired amount of Rh–TA (0.3, 0.5, and 1.0 mol.% based on AMPS amounts) was emulsified in 4 mL water with sonication. AMPS (1.00 g, 4.83 mmol), NMBA (0.03 g, 0.19 mmol), 1 wt% catalyst aqueous solution of TEMED (0.145 mL, 0.010 mmol), and 10 wt% initiator aqueous solution of APS (0.165 mL, 0.072 mmol) were further added into the emulsified solution. The reaction mixture was injected in the aforementioned reaction holder and crosslinked at 50 °C for few hours. Therefore, three Rh–SN samples (i.e., Rh0.3–SN, Rh0.5–SN, and Rh1.0–SN) were obtained.

Synthesis of Rh-containing DN (Rh–DN) hydrogels (i.e., Scheme 1B2). Rh–SNs were individually immersed in a mixture with DMAA (3.13 mL, 30.40 mmol), AA (0.23 mL, 3.83 mmol), APS (0.099 g, 0.434 mmol), and water (12 mL). We then proceeded with a similar procedure for the 2nd network of Rh–DN hydrogel. Eventually, different amounts of Rh-containing DN hydrogels were obtained (i.e., Rh0.3–DN, Rh0.5–DN, and Rh1.0–DN) and used with high water contents.

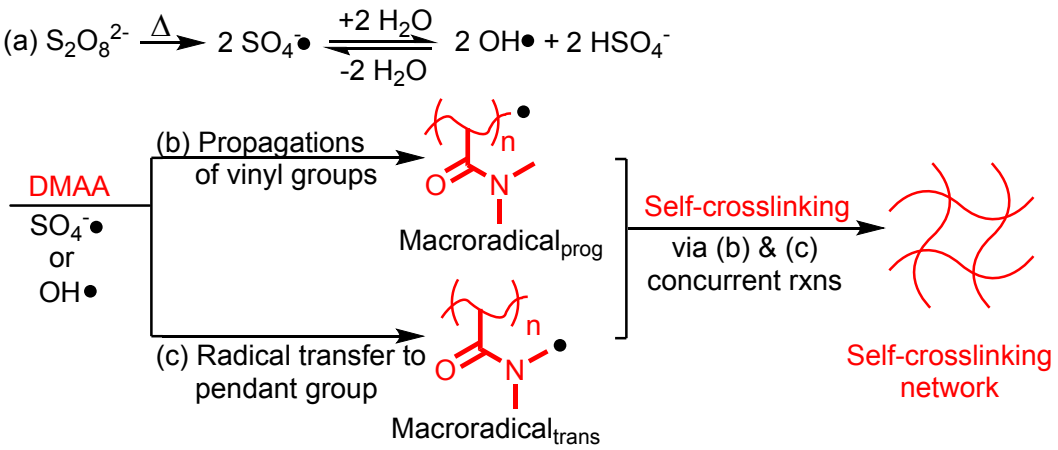

Scheme S1. Proposed self-crosslinking mechanism of APS/DMAA through (a) thermal/redox initiations and (b) propagations (prog)/(c) radical transfer (trans) concurrent reactions.

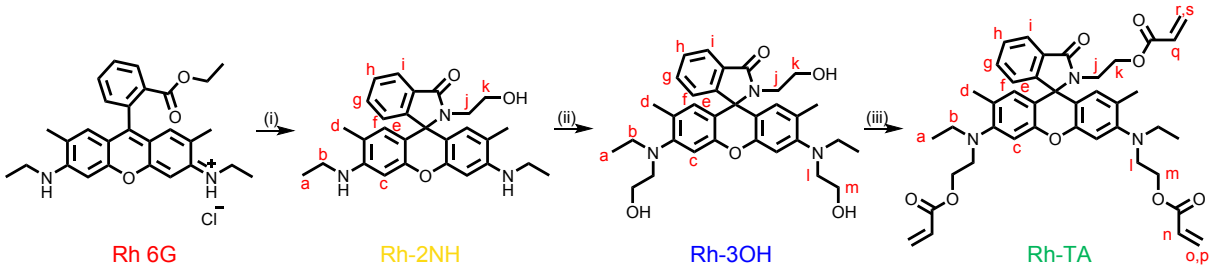

Scheme S2. Synthetic routs from Rh 6G, Rh–2NH, Rh–3OH to Rh–TA derivatives [(i) 2-aminoethan-1-ol, reflux in MeCN for 2 h (yield: 65%), (ii) 2-chloroethanol and K_2CO_3 at 100 °C for overnight (yield: 67%), and (iii) acryloyl chloride and triethyl amine in DCM, 25 °C for a day (yield: 95%)].

Table S1. Thermal properties of (Rh–)DN dried samples.

Sample	T_g (°C)	ΔT_g (°C)[a]	$T_{d5\%}$ (°C)[b]	Char Yield (%)
DN	143.9	38.6	289.2	17.3
Rh0.3-DN	135.7	34.3	283.9	18.0
Rh0.5-DN	137.0	50.4	286.5	16.2
Rh1.0-DN	137.8	51.6	284.1	17.0

[a] $\Delta T_g \equiv (T_{g,\,onset} - T_{g,\,end})$, determined from DSC profiles.

[b] $T_{d5\%}$: temperatures of 5 wt% loss of the samples, determined from TGA thermograms.

Table S2. Summary of tensile/compression stress at break (σ_{Tb}/σ_{Cb})–tensile/compression strain at break ($\varepsilon_{Tb}/\varepsilon_{Cb}$) results.

	Tensile (T) results				Compression (C) results			
	σ_{Tb} (kPa)	ε_{Tb} (%)	E_T† (MPa)	U_T§ (kJ/m^3)	σ_{Cb} (MPa)	ε_{Cb} (%)	E_C‡ (MPa)	U_C§ (kJ/m^3)
DN	590.15	123.7	0.68	449.9	4.75	63.5	15.6	748.3
Rh0.3-DN	459.69	86.5	0.56	196.9	1.70	72.5	4.7	254.6
Rh0.5-DN	486.25	60.9	0.79	126.5	2.38	53.7	9.7	377.6
Rh1.0-DN	556.41	37.5	1.50	92.2	2.65	51.8	11.2	403.2

† E_T (tensile modulus): estimated from the slopes of the curves before breaking elongations of 50%.

§ U_T: tensile fracture energy and U_C: compression fracture energy.

‡ E_C (compression modulus): estimated from the slopes of the curves before breaking compressions of 40%.

Table S3. Summary of CIE coordinates (i.e., x;y values) with various compression stresses.

Sample	0 MPa	0.5 MPa	1.0 MPa	1.5 MPa	1.6 MPa	2.0 MPa	2.6 MPa
Rh0.3-DN	0.317;0.333	0.323;0.331	0.334;0.337	0.339;0.334	0.335;0.330	n.d.†	n.d.
Rh0.5-DN	0.322;0.334	0.335;0.328	0.343;0.333	0.366;0.329	n.d.	0.379;0.328	n.d.
Rh1.0-DN	0.327;0.342	0.342;0.330	0.377;0.325	0.372;0.326	0.393;0.323	0.412;0.312	0.438;0.312

† n.d.: non-detective results.

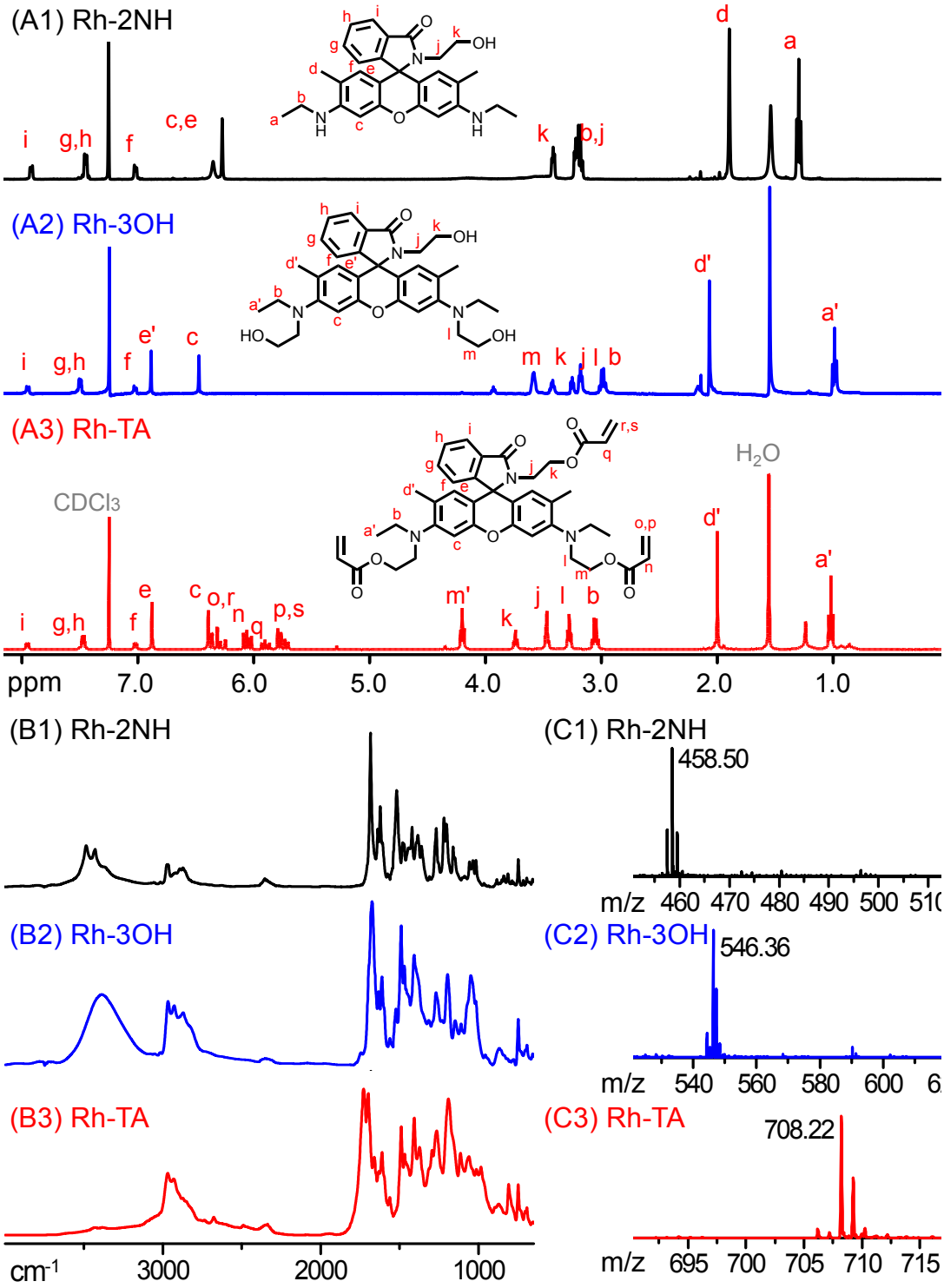

Figure S1. (A) ^{1}H NMR (400 MHz, $CDCl_3$), (B) FT-IR (4000–600 cm^{-1}) spectra, and (C) MALDI-TOF MS spectra of (1) Rh–2NH, (2) Rh–3OH, and (3) Rh–TA derivatives.

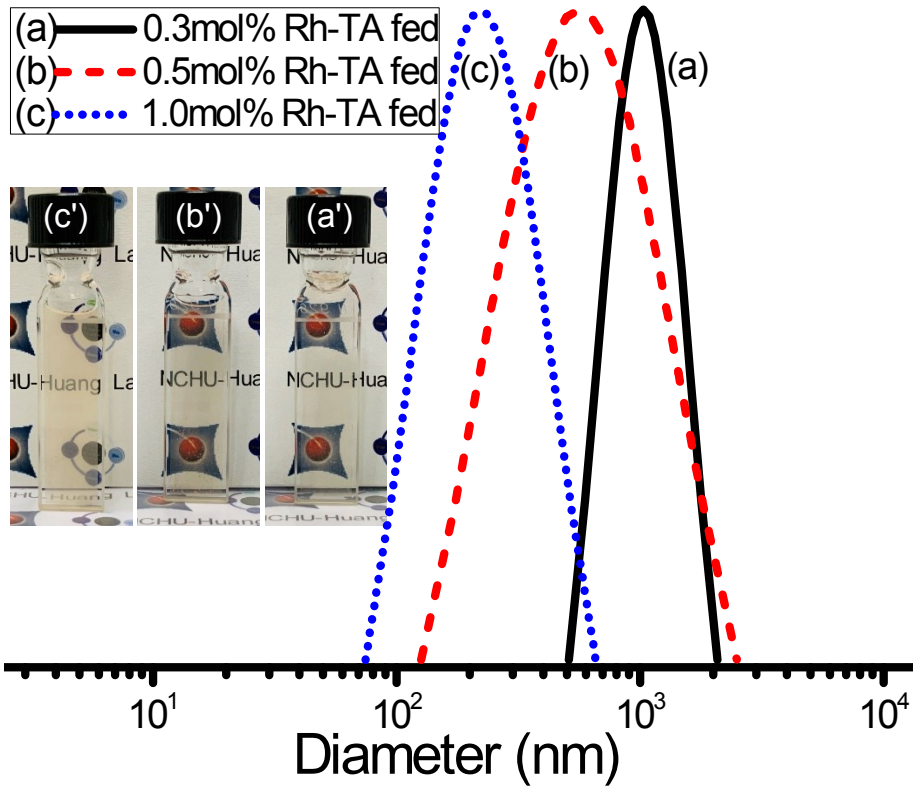

Figure S2. Images of emulsified solutions (inserted figures a'–c') and the corresponding DLS analysis (a–c) with 0.3, 0.5, and 1.0 mol% of Rh–TA in feed (based on AMPS monomer).

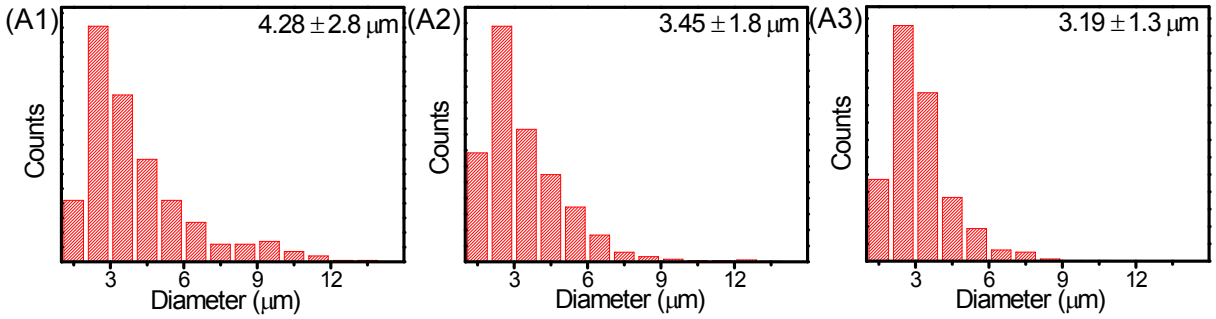

Figure S3. Estimated pore size distributions from the corresponding Cryo-SEM images in Figure 1A of Rh-containing single network hydrogels: (A1) Rh0.3–SN, (A2) Rh0.5–SN, and (A3) Rh1.0–SN.

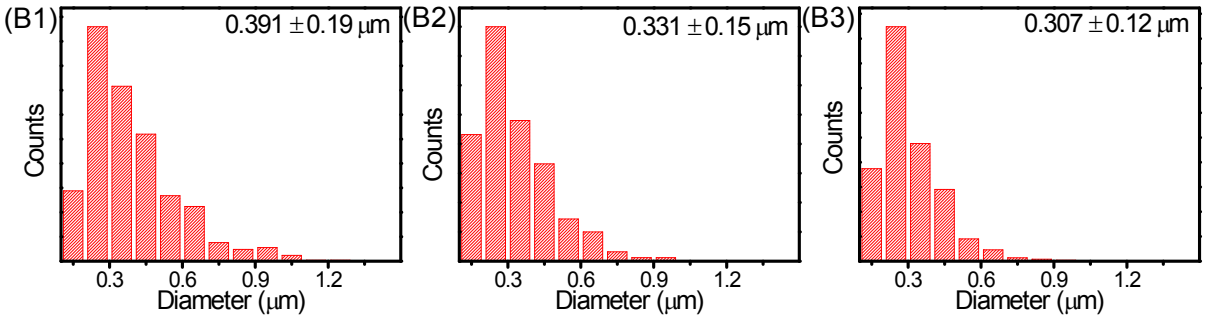

Figure S4. Estimated pore size distributions from the corresponding Cryo-SEM images in Figure 1B of Rh-containing double network hydrogels: (B1) Rh0.3–DN, (B2) Rh0.5–DN, and (B3) Rh1.0–DN.

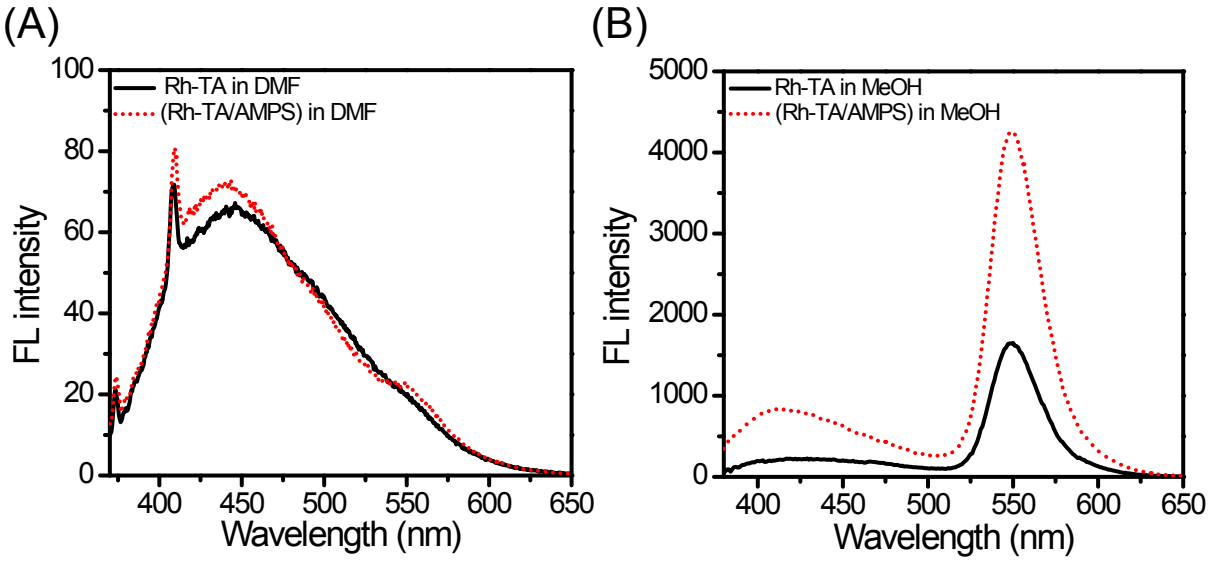

Figure S5. Fluorescence spectra of (A) Rh–TA (200 μM) in DMF and (B) Rh–TA (20 μM) MeOH with and without of AMPS monomer (20 mM).

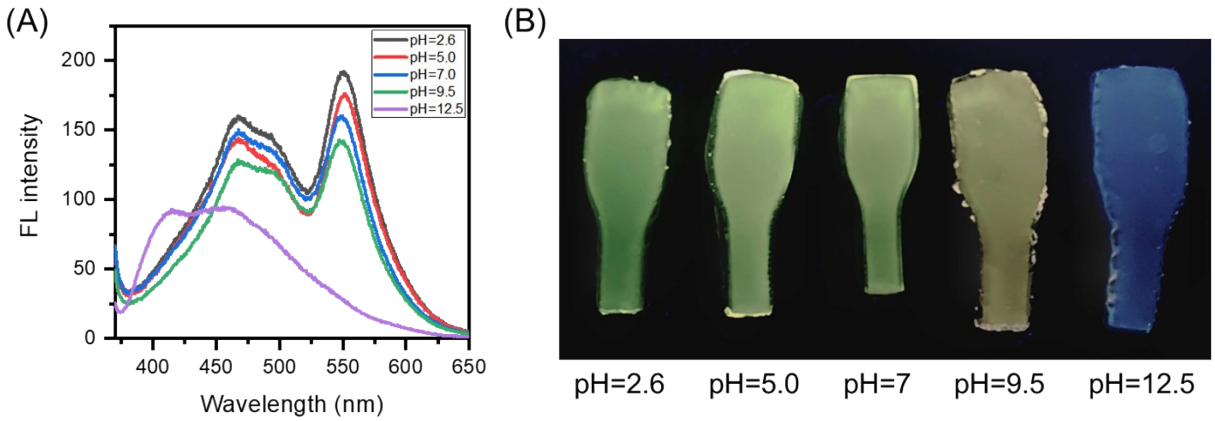

Figure S6. (A) Fluorescence (FL) spectra and (B) emission colours of Rh1.0–DN (under UV light, λ = 365 nm) after immersing in different pH aqueous for a day.

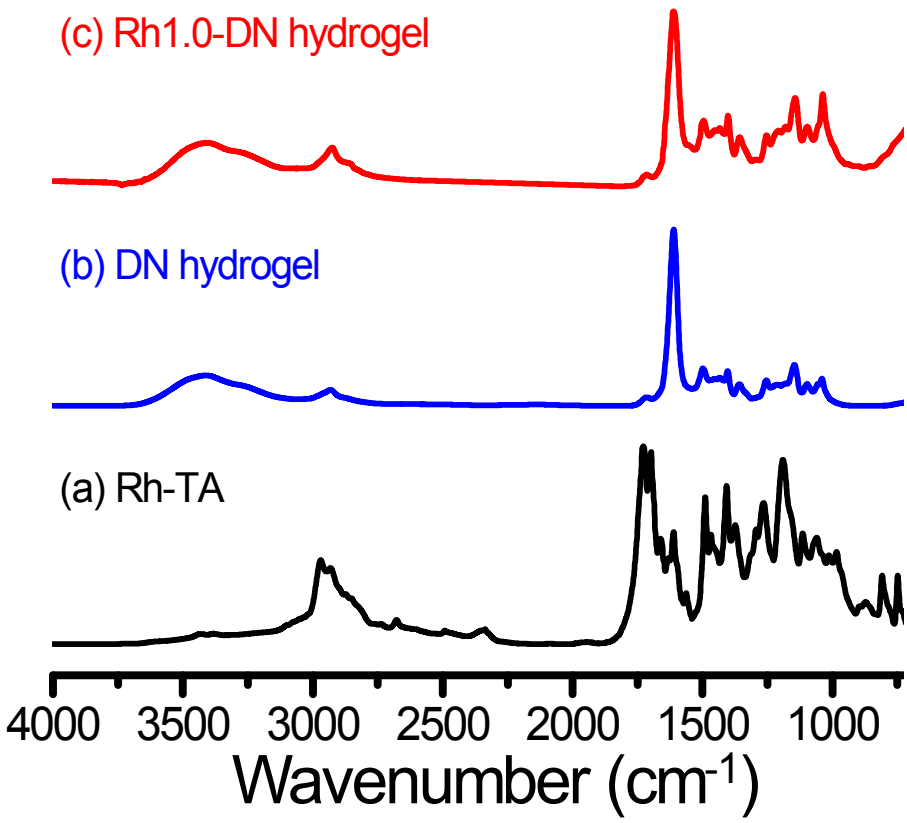

Figure S7. FT-IR (4000–750 cm^{-1}) spectra of (a) Rh–TA, (b) DN, and (c) Rh1.0–DN dried samples.

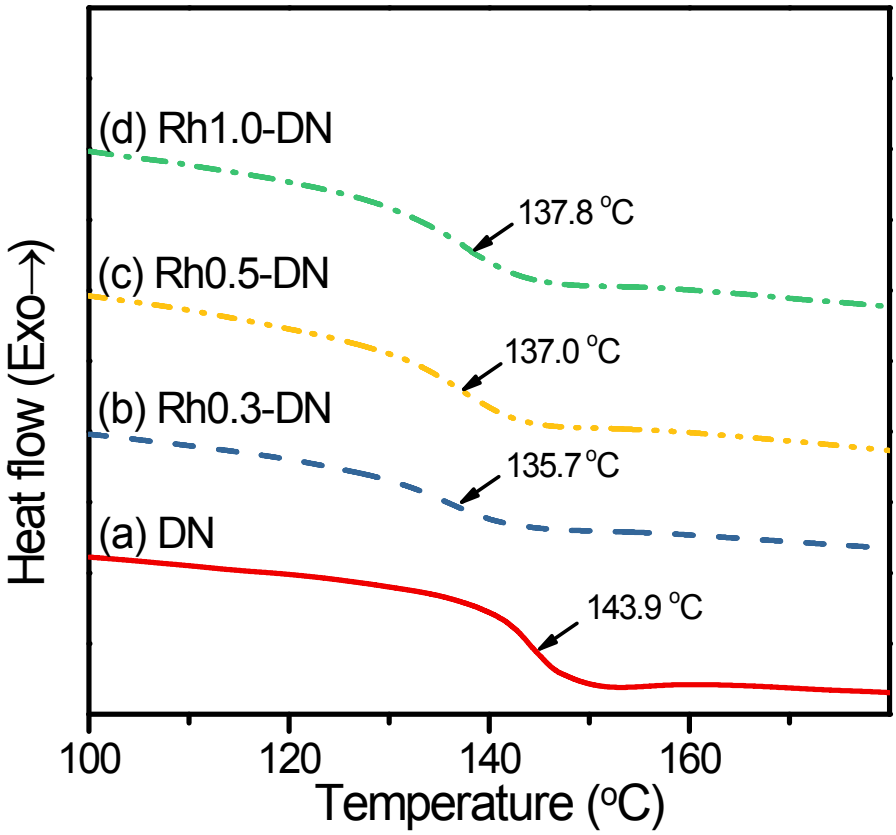

Figure S8. DSC profiles of (a) DN, (b) Rh0.3–DN, (c) Rh0.5–DN, and (d) Rh1.0–DN dried samples (ramp: 20 °C/min; range: 100–180 °C under $N_{2(g)}$).

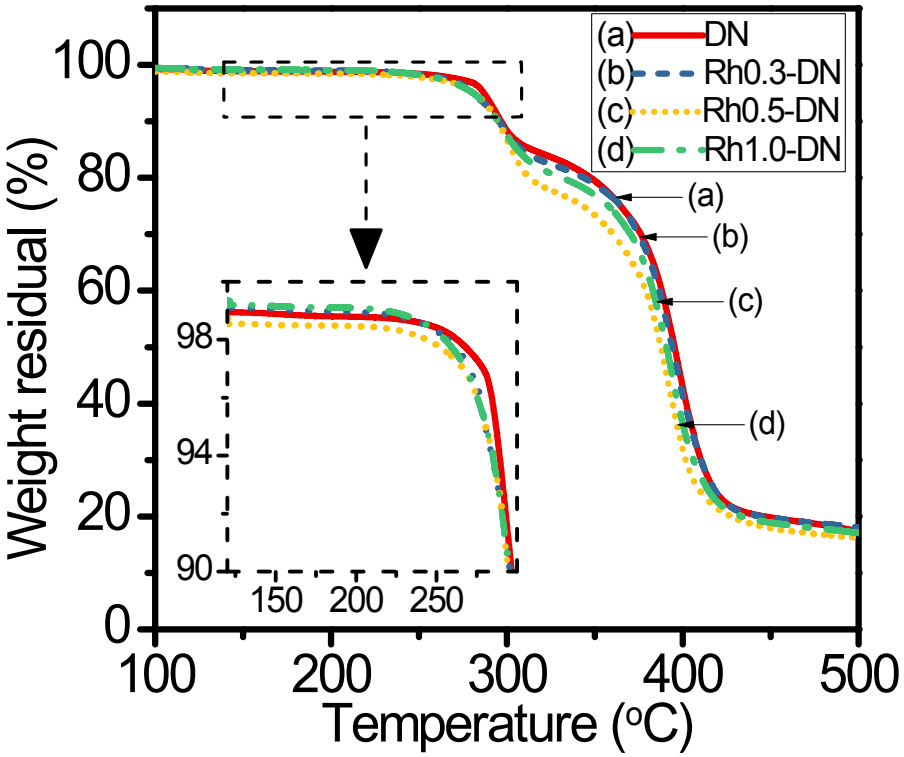

Figure S9. TGA thermograms of (a) DN, (b) Rh0.3–DN, (c) Rh0.5–DN, and (d) Rh1.0–DN dried samples (ramp: 20 °C/min; range: 100–500 °C under $N_{2(g)}$; inserted figure: range: 140–300 °C).

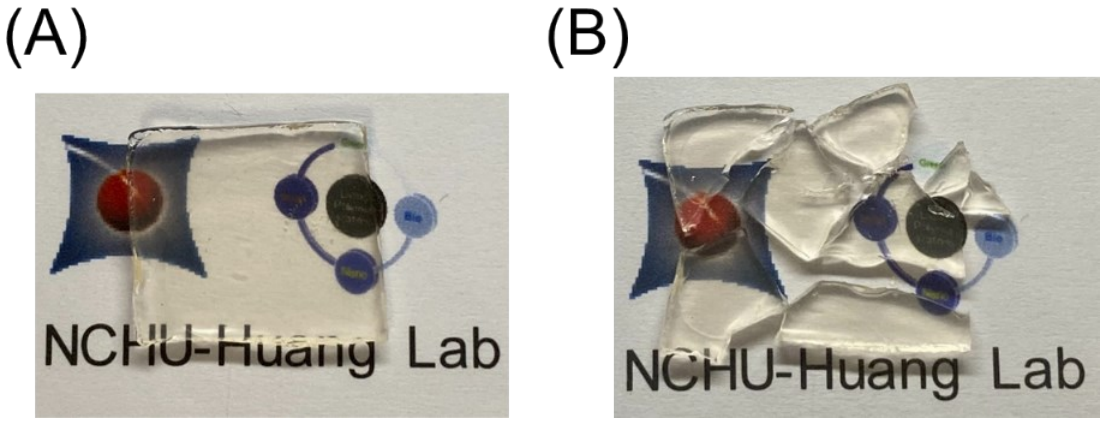

Figure S10. Photographs of (A) before and (B) after compressing Rh1.0–SN hydrogels.

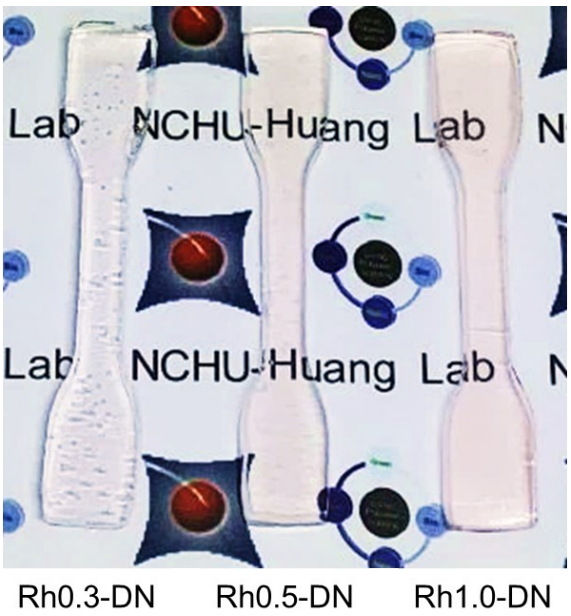

Figure S11. Appearances of the pristine Rh0.3–DN, Rh0.5–DN, and Rh1.0–DN hydrogels.

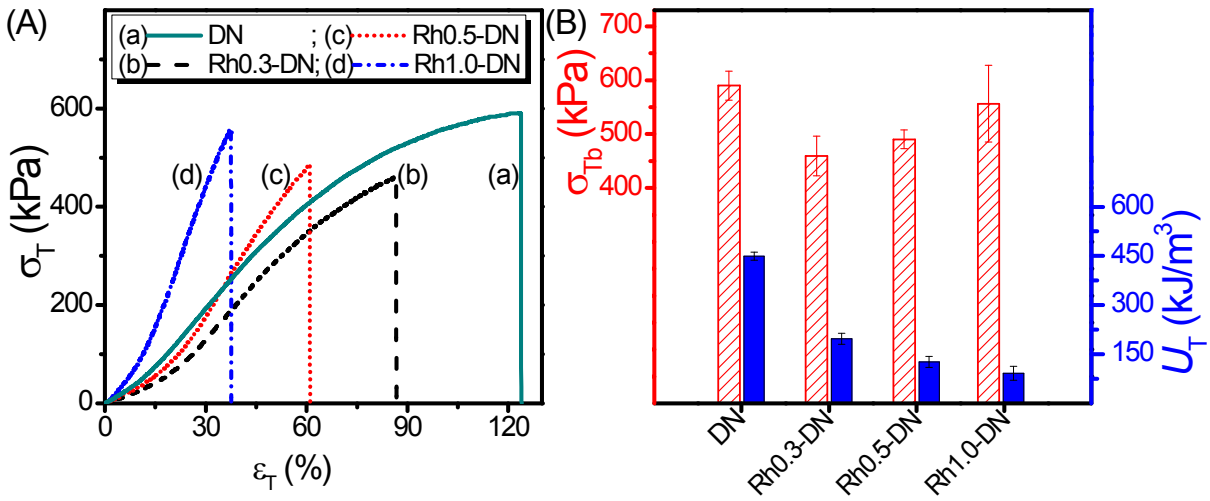

Figure S12. (A) Tensile stress vs strain curves and (B) the corresponding results of various DN hydrogels (σ_T: tensile stress (kPa), ε_T: tensile strain (%), σ_{Tb}: tensile strength at break (kPa), and U_T (kJ/m^3): tensile fracture energy).

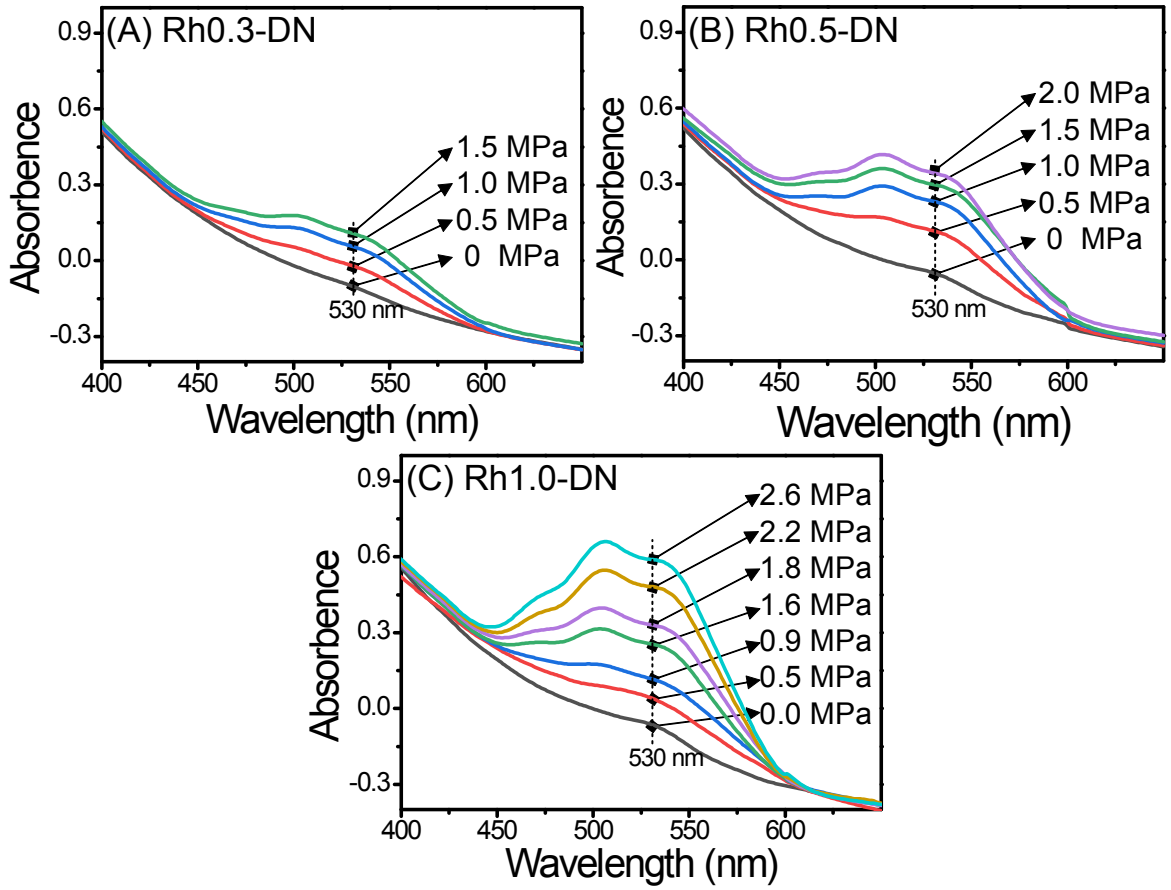

Figure S13. UV–Vis traces with various compression stress (MPa) of (A) Rh0.3–DN, (B) Rh0.5–DN, and (C) Rh1.0–DN hydrogels.

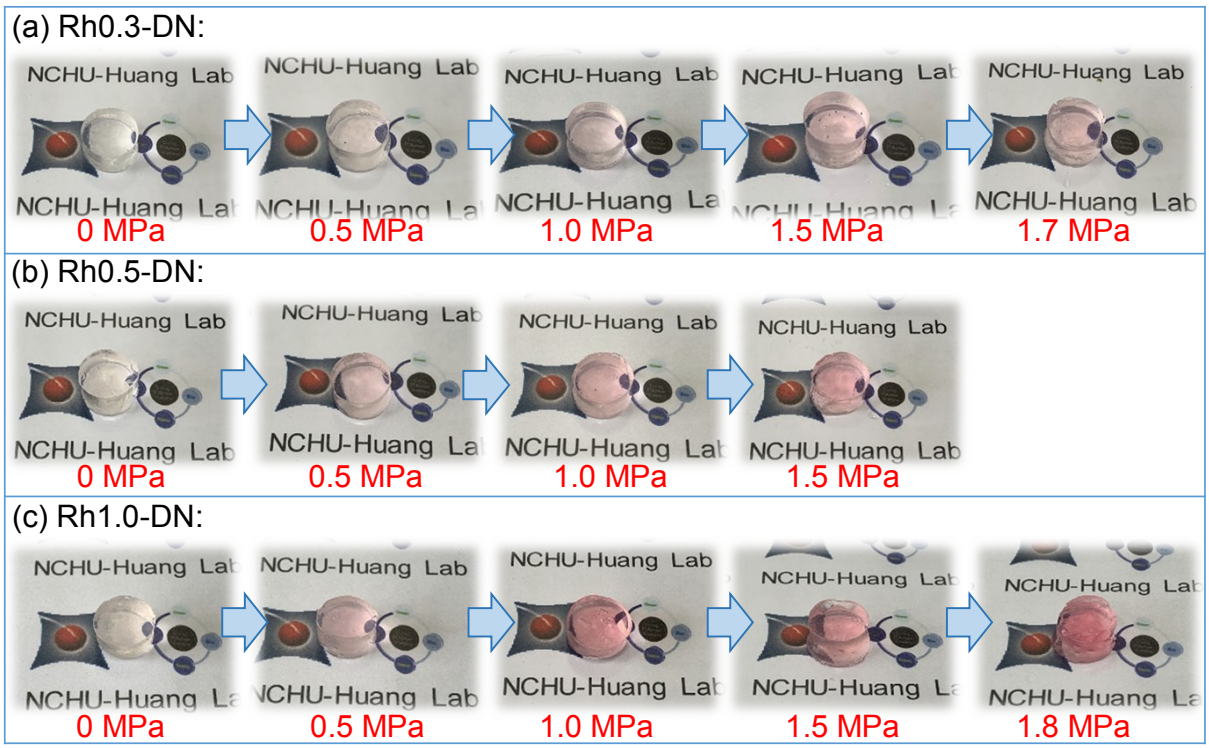

Figure S14. Apparent colour changes of (a) Rh0.3–DN, (b) Rh0.5–DN, and (c) Rh1.0–DN specimens with various compression stresses.

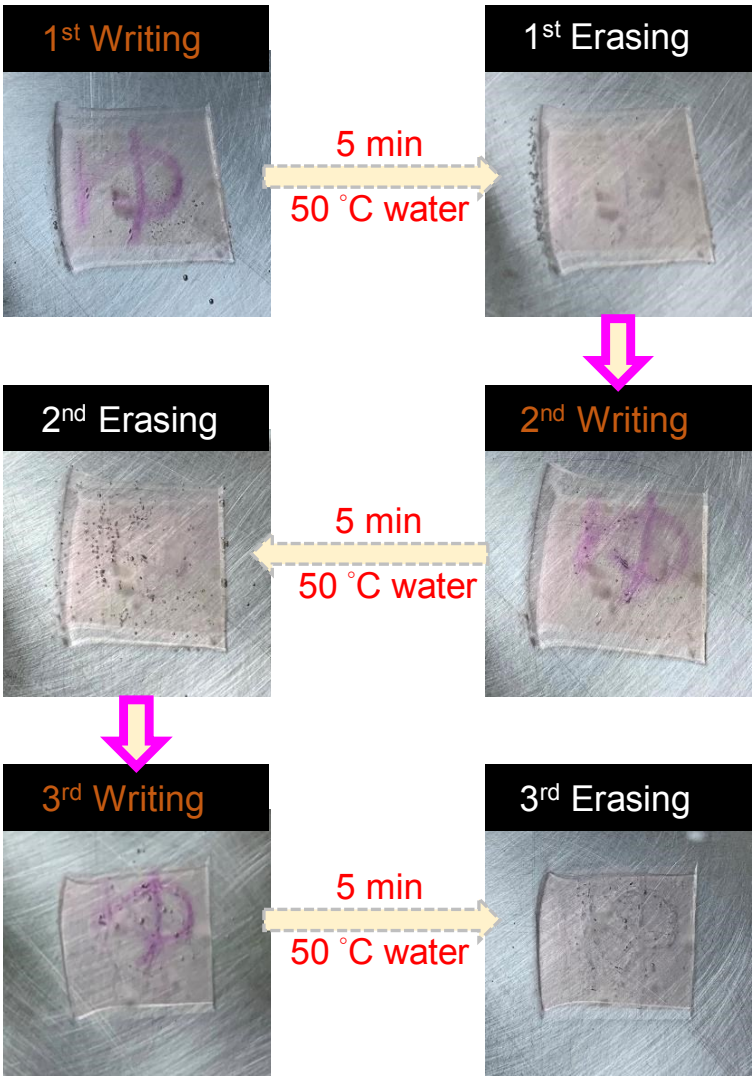

Figure S15. Apparent reversibility of Rh1.0–DN sample through "Writing-Erasing" cycles (i.e., writing by hand pressing; erasing by immersing in 50 °C water for 5 min).